

Article

Synthesis and Structure-Activity Relationships of LP1 Derivatives: *N*-Methyl-*N*-phenylethylamino Analogues as Novel MOR Agonists

Rita Turnaturi ¹ , Carmela Parenti ², Orazio Prezzavento ¹, Agostino Marrazzo ¹ ,
Paschalina Pallaki ³, Zafiroula Georgoussi ³, Emanuele Amata ¹ and Lorella Pasquinucci ^{1,*} 

¹ Department of Drug Sciences, Medicinal Chemistry Section, University of Catania, Viale A. Doria 6, 95125 Catania, Italy; rita.turnaturi@unict.it (R.T.); prezzave@unict.it (O.P.); marrazzo@unict.it (A.M.); eamata@unict.it (E.A.)

² Department of Drug Sciences, Pharmacology and Toxicology Section, University of Catania, Viale A. Doria 6, 95125 Catania, Italy; cparenti@unict.it

³ Laboratory of Cellular Signaling and Molecular Pharmacology, Institute of Biosciences and Applications, National Centre for Scientific Research “Demokritos” Agia Paraskevi-Attikis, 15310 Athens, Greece; ppallaki@bio.demokritos.gr (P.P.); iro@bio.demokritos.gr (Z.G.)

* Correspondence: lpasquin@unict.it; Tel.: +39-095-738-4273

Received: 21 February 2018; Accepted: 15 March 2018; Published: 16 March 2018

Abstract: The opioid pharmacological profile of *cis*(-)-*N*-normetazocine derivatives is deeply affected by the nature of their *N*-substituents. Here, our efforts were focused on the synthesis and pharmacological evaluation of novel derivatives of the lead LP1, a multitarget opioid analgesic compound featuring an *N*-phenylpropanamido substituent. LP1 derivatives **5a–d** and **6a–d** were characterized by flexible groups at the *N*-substituent that allow them to reposition themselves relative to *cis*(-)-*N*-normetazocine nucleus, thus producing different pharmacological profiles at the mu, delta and kappa opioid receptors (MOR, DOR and KOR) in in vitro and in vivo assays. Among the series, compound **5c**, with the best in vitro and in vivo profile, resulted a MOR agonist which displays a K_i^{MOR} of 6.1 nM in a competitive binding assay, and an IC_{50} value of 11.5 nM and an I_{max} of 72% in measurement of cAMP accumulation in HEK293 cells stably expressing MOR, with a slight lower efficacy than LP1. Moreover, in a mouse model of acute thermal nociception, compound **5c**, intraperitoneally administered, exhibits naloxone-reversed antinociceptive properties with an ED_{50} of 4.33 mg/kg. These results expand our understanding of the importance of *N*-substituent structural variations in the opioid receptor profile of *cis*(-)-*N*-normetazocine derivatives and identify a new MOR agonist useful for the development of novel opioid analgesics for pain treatment.

Keywords: 6,7-benzomorphan derivatives; MOR agonist; pain; radioligand competitive binding; cAMP accumulation assay; tail-flick test

1. Introduction

The *cis*(-)-*N*-normetazocine nucleus, derived by structure-activity relationships (SARs) during morphine skeleton simplification [1,2], has been the subject of medicinal chemistry exploration for the development of new drugs and pharmacological tools to explore opioid pharmacology in vitro and in vivo [3]. This nucleus is a rigid scaffold able to support the phenolic ring and the basic nitrogen in a correct conformation mimicking the tyramine of opioid peptides [4]. A plethora of experimental evidence demonstrated the unpredictability of agonist and antagonist properties conferred by *N*-substituents on 6,7-benzomorphan ligands [5–9]. Thus, our approach consisted in the introduction at the basic nitrogen of the *cis*(-)-*N*-normetazocine nucleus of different functional

groups with the aim to explore their influence on the mu, delta and kappa opioid receptor (MOR, DOR and KOR) affinity, selectivity and activity in the resulting compounds.

Previously, we synthesized a series of compounds by introducing at the *N*-substituent of *cis*-(-)-*N*-normetazocine an aromatic ring and/or alkyl residues linked by an *N*-propanamido or *N*-acetamido spacers (Figure 1) [10]. Among them, the multitarget opioid ligand LP1, featured by an *N*-phenylpropanamido substituent, possessed affinity and intrinsic activity for MOR ($K_i = 0.83$ nM, $IC_{50} = 4.8$ nM) and DOR ($K_i = 29.1$ nM, $IC_{50} = 12$ nM). LP1, *in vivo* tested, resulted a potent opioid analgesic compound ($ED_{50} = 2.03$ mg/kg) with low tolerance-inducing capability [11,12] also suitable for the management of persistent pain conditions such as neuropathic and inflammatory pain [13].

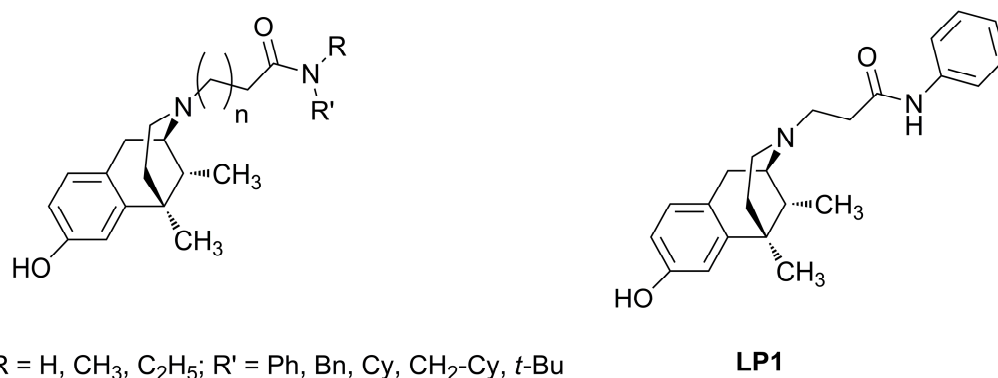


Figure 1. Structures of LP1 and its analogues.

Here, our efforts were focused on the evaluation of the effect of *N*-substituent structural variations on the opioid receptor profile of LP1 through the design and synthesis of two new series of derivatives. The new LP1 derivatives designed possessed different secondary and tertiary ethylamino or propylamino side chains bearing phenyl or cyclohexyl rings (Figure 2). Thus, they may help our understanding of opioid ligand-receptor interactions. All synthesized LP1 derivatives were tested by opioid receptor competitive binding assays to determine their affinity at MOR, DOR and KOR. Moreover, the compounds were further evaluated *in vitro* by measuring their adenylyl cyclase (AC) activity in order to establish their functional profile. Finally, the compound with the best functional profile was also tested *in vivo* through a mouse tail flick test.

In the new synthesized benzomorphan ligands flexible groups at the *N*-substituent position allow them to reposition themselves relative to the *cis*-(-)-*N*-normetazocine nucleus thus producing a different pharmacological profile at MOR, DOR and KOR. In particular, compound 5c, with the best *in vitro* and *in vivo* profile, resulted a MOR agonist suitable for the development of novel analgesic drugs.

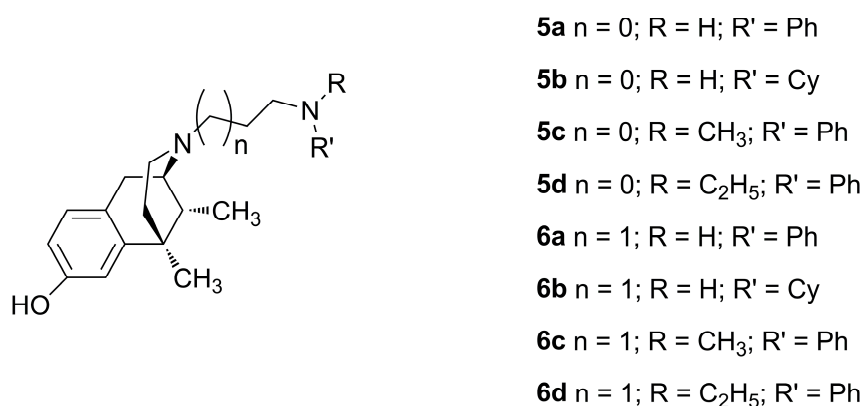
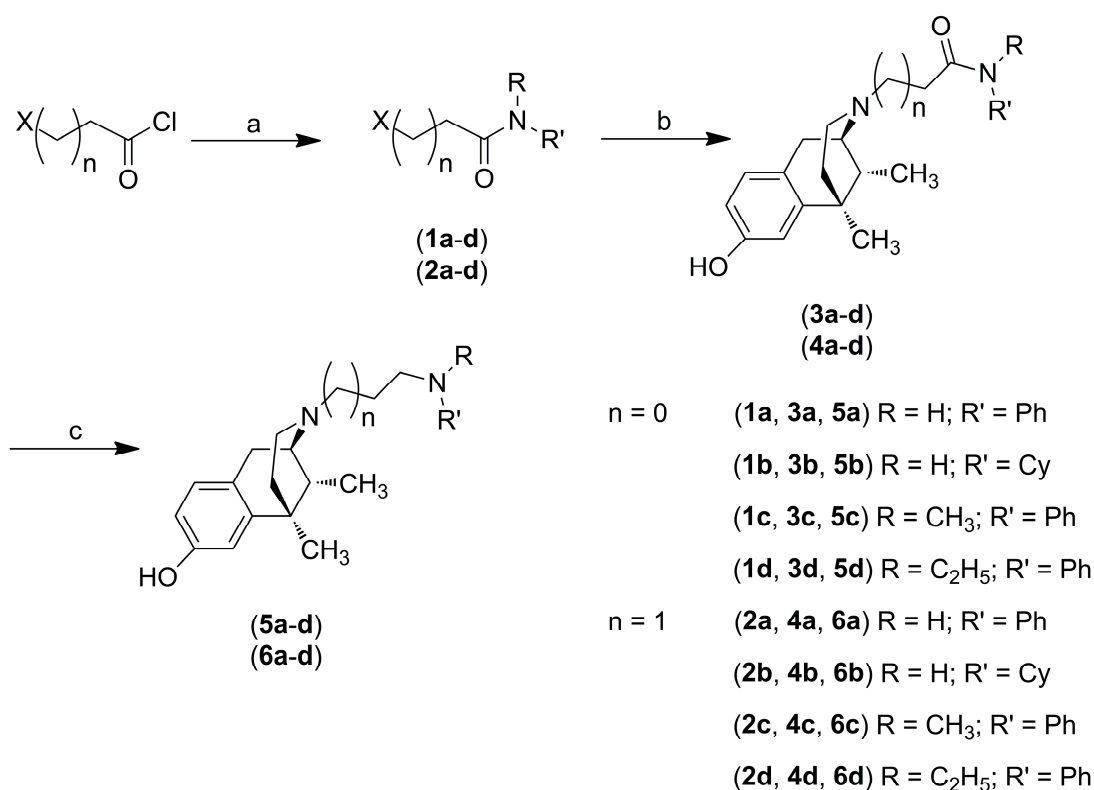


Figure 2. Structures of LP1 *N*-modified derivatives 5a–d and 6a–d.

2. Results and Discussion

2.1. Chemistry

The synthesis of the novel compounds **5a–d** and **6a–d** was carried out as illustrated in Scheme 1. Amides **1a–d** and **2a–d** were prepared by acylation of the respective amines with 2-chloroacetyl chloride and 3-bromopropionyl chloride, respectively, and compounds **3a–d** and **4a–d** were obtained by alkylation of *cis*-(-)-(1*R*,5*R*,9*R*)-*N*-normetazocine with the respective amides, as previously reported [10,14]. Then, reduction of compounds **3a–d** and **4a–d** with diborane in anhydrous THF provided the final compounds **5a–d** and **6a–d**. The new synthesized derivatives were characterized by IR, ¹H-NMR, ¹³C-NMR and elemental analysis.



Reagents and conditions: a) Respective amine, DMAP, THF, 0 °C, 1h; b) (-)-*cis*-(1*R*,5*R*,9*R*)-*N*-normetazocine, NaHCO₃, KI, DMF, 50 °C, 12h; c) Diborane, THF, reflux, 12h.

Scheme 1. Synthetic pathway.

2.2. Pharmacology

2.2.1. In Vitro Radioligand Binding Assay

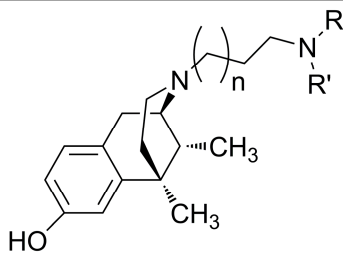
The MOR, DOR and KOR binding affinity of compounds **5a–d** and **6a–d** were determined by radioligand competitive binding experiments as previously reported [15]. Calculated inhibition constant (K_i) values are listed in Table 1.

As shown in Table 1, LP1 derivatives displayed a broad range of binding affinity for MOR (K_i = 6.1–160 nM) and KOR (K_i = 19.8–56 nM) and lesser or no affinity towards DOR. The first series of ligands **5a–d**, with an *N*-ethylamino spacer, retained a significant MOR affinity, in particular **5c** and **5b**, although in comparison to the lead LP1 their K_i values were 7- and 10-times higher. With the exception of compound **5a**, an improved KOR affinity was reported for compounds **5b–d**. Indeed, their K_i values

were 5-, 3- and 4-times lower than the LP1 K_i value. A worse DOR affinity profile was recorded for compounds **5a–d**.

For the second series of ligands **6a–d**, with an *N*-propylamino side chain, a similar trend of affinity was recorded. The binding profile of compounds **6a–d** versus MOR got worse, and in fact their K_i values were 10-, 58-, 82- and 103 times higher in comparison to LP1. In addition, in comparison with the series containing the *N*-ethylamino substituent, the K_i values of compounds **6a–d** for MOR were higher. Analogously to the series **5a–d**, an improved KOR binding affinity was recorded also for the series with the *N*-propylamino substituent **6a–d**. Their K_i values for KOR were lower in comparison to LP1 and higher in comparison to the series **5a–5d**. The introduction of the *N*-propylamino substituent was significantly detrimental for DOR binding affinity.

Table 1. Opioid receptor binding affinity of compounds **5a–d** and **6a–d**.



| Compound | n | R | R' | K_i (nM) \pm SEM ^{a,b} | | |
|-------------|---|-------------------------------|--------------------------------|-------------------------------------|----------------|----------------|
| | | | | MOR | DOR | KOR |
| 5a | 0 | H | Ph | 83 \pm 30 | 270 \pm 10 | 100 \pm 5.0 |
| 5b | 0 | H | C ₆ H ₁₁ | 8.3 \pm 0.8 | 70 \pm 2.0 | 19.8 \pm 0.9 |
| 5c | 0 | CH ₃ | Ph | 6.1 \pm 0.5 | 147 \pm 5.7 | 31 \pm 1.3 |
| 5d | 0 | C ₂ H ₅ | Ph | 160 \pm 7.0 | 411 \pm 14 | 28.7 \pm 1.0 |
| 6a | 1 | H | Ph | 7.0 \pm 0.6 | 117 \pm 5.2 | 71 \pm 2.0 |
| 6b | 1 | H | C ₆ H ₁₁ | 48 \pm 1.4 | >5000 | 126 \pm 4.5 |
| 6c | 1 | CH ₃ | Ph | 68 \pm 1.6 | >5000 | 94 \pm 3.5 |
| 6d | 1 | C ₂ H ₅ | Ph | 86 \pm 3.0 | 1060 \pm 152 | 56 \pm 1.7 |
| LP1 | | | | 0.83 \pm 0.05 | 29.1 \pm 1.0 | 110 \pm 6.0 |
| DAMGO | | | | 1.16 \pm 0.1 | - | - |
| U50,488 | | | | - | - | 0.34 \pm 0.1 |
| Naltrindole | | | | - | 1.13 \pm 0.1 | - |

^a Values are means \pm SEM of three separate experiments, each carried out in duplicate. ^b K_i values were obtained as [³H]DAMGO displacement for MOR, [³H]DPDPE displacement for DOR, and [³H]U69,593 displacement for KOR.

In general, in *N*-amino derivatives **5a–d** and **6a–d** the introduction of a second positive charge at the nitrogen substituent retained MOR affinity, improved KOR affinity and dramatically reduced DOR affinity. Among the series, compounds **5b** and **5c**, with the *N*-cyclohexylethylamino and *N*-methyl-*N*-phenylethylamino substituent, respectively, showed a significant MOR (K_i = 8.3 and 6.1 nM, respectively) and KOR (K_i = 19.8 and 31 nM, respectively) affinity and the compound **6a**, with the *N*-phenylpropanamino substituent, showed similar MOR/KOR binding values of compounds **5b** and **5c** (Table 1).

In comparison to the respective previously synthesized and in vitro evaluated *N*-amido series (Figure 1), an opposite trend emerged [10]. Indeed, the shorter *N*-acetamido spacer produced a significant loss of MOR affinity relative to their *N*-propanamido homologs. All *N*-acetamido and *N*-propanamido compounds displayed a low KOR affinity with the partial exception of the compound bearing the *N*-ethyl-*N*-phenylpropanamido substituent (K_i^{KOR} = 70 nM). Moreover, the *N*-secondary amido substituent was preferred for MOR interaction while the *N*-tertiary amido substituent was unfavorable. These evidences suggested that, in comparison to the *N*-acetamido and *N*-propanamido series, the increased flexibility of *N*-substituent of compounds **5a–d** and **6a–d** and the presence of a

second positive charge could allow a different interaction with the opioid receptor binding pocket. In fact, all new synthesized compounds possess orientable groups at the *N*-substituent that allow to reposition themselves relative to the *cis*-(-)-*N*-normetazocine nucleus giving differences in binding versus MOR, DOR and KOR.

2.2.2. Adenylyl Cyclase-Mediated Effects

As typical G_i/o coupled receptor, MOR, DOR and KOR signals are mediated by AC inhibition. Given the significant MOR and moderate KOR affinity, to examine the functional role of target compounds, in opioid receptor signaling, the ability of **5a–d** and **6a–d** to affect forskolin-stimulated AC activity in HEK293 cells stably expressing the MOR or KOR was tested and the results are reported in Table 2.

Table 2. Effect of compounds **5a–d** and **6a–d** on cAMP accumulation by the KOR and MOR.

| Compound | IC ₅₀ (nM) ± SD ^{a,b} | | I _{max} (%) ± SD ^c | |
|----------------|---|-----------------|--|--------|
| | MOR | KOR | MOR | KOR |
| 5a | 55.3 ± 7.0 | 1000 ± 65 | 60 ± 4 | - |
| 5b | 74.0 ± 3.5 | 180 ± 50 | 28 ± 1 | 58 ± 4 |
| 5c | 11.5 ± 2.5 | ND ^d | 72 ± 5 | - |
| 5d | 66 ± 1.3 | ND | 55 ± 3 | - |
| 6a | 7.4 ± 1.1 | 1400 ± 69 | 50 ± 3 | 53 ± 4 |
| 6b | ND | >5000 | - | 44 ± 3 |
| 6c | 21.61 ± 3.5 | ND | 50 ± 3 | - |
| 6d | 9.51 ± 2.0 | ND | 40 ± 2 | - |
| LP1 | 4.8 ± 0.5 | - | 73 ± 3.8 | - |
| DAMGO | 3.18 ± 0.3 | - | 73 ± 0.3 | - |
| U50,488 | | 0.82 ± 0.03 | | 68 ± 5 |

^a Agonist properties of compounds in the inhibition of forskolin-stimulated cAMP accumulation by MOR and KOR. The inhibition of cAMP accumulation was measured as described in Section 4.3. ^b IC₅₀ value is the concentration of the compound needed to produce half maximal inhibition, with all values presented as the average ± SD of triplicate determinations from three independent experiments. ^c IC_{max} value is the maximal percent inhibition obtained with the compound. ^d ND, not determined.

In HEK293 cells stably expressing the MOR, compounds **5a–d** and **6a–d**, with the exception of compound **6b**, dose-dependently inhibited cAMP accumulation although with marked differences in potency and efficacy. Compound **5c** resulted a MOR agonist that, in comparison to LP1, showed a 2-times higher IC₅₀ value but comparable efficacy. Compounds **5a, b, d** and **6a, c, d** resulted weak MOR partial agonists with IC₅₀ values ranging from 7.4 nM to 74.0 nM and I_{max} values ranging from 28% to 60% inhibition over control. In parallel experiments in HEK293 cells stably expressing KOR, target compounds exhibited a different trend. In particular, **5a,b** and **6a,b** showed a very low potency, with IC₅₀ values ranging from 180 nM to 5000 nM, and efficacy with I_{max} values ranging from 44% to 58% inhibition over control. Compounds **5c,d** and **6c,d** were not able to dose-dependently inhibit cAMP accumulation and only at very high concentrations determined 30% cAMP inhibition.

2.2.3. Tail Flick Test

The MOR agonist **5c** was evaluated for acute agonistic effects in mice. In detail, it was tested for its ability to produce antinociception in the mouse tail flick test at the dose-range of 1–7 mg/kg intraperitoneal (ip) injected. The compound produced a dose-dependent analgesic effect compared to the group of mice treated with saline (* *p* < 0.05 vs. saline-treated mice). In vivo evaluation of **5c** established that the maximal antinociceptive activity was reached at 45 min (Figure 3, panel A) after ip injection and significantly lasted, at the highest dose, until 75 min after injection. Pretreatment with naloxone (3 mg/kg sc), 30 min prior to **5c**, prevented its antinociceptive effect (data not shown). Figure 3, panel B shows the analgesic dose-response curve with the ED₅₀ value (4.33 mg/kg ip) and its confidence limits (CL) (3.35–5.59). These results are in agreement with our in vitro functional assays.

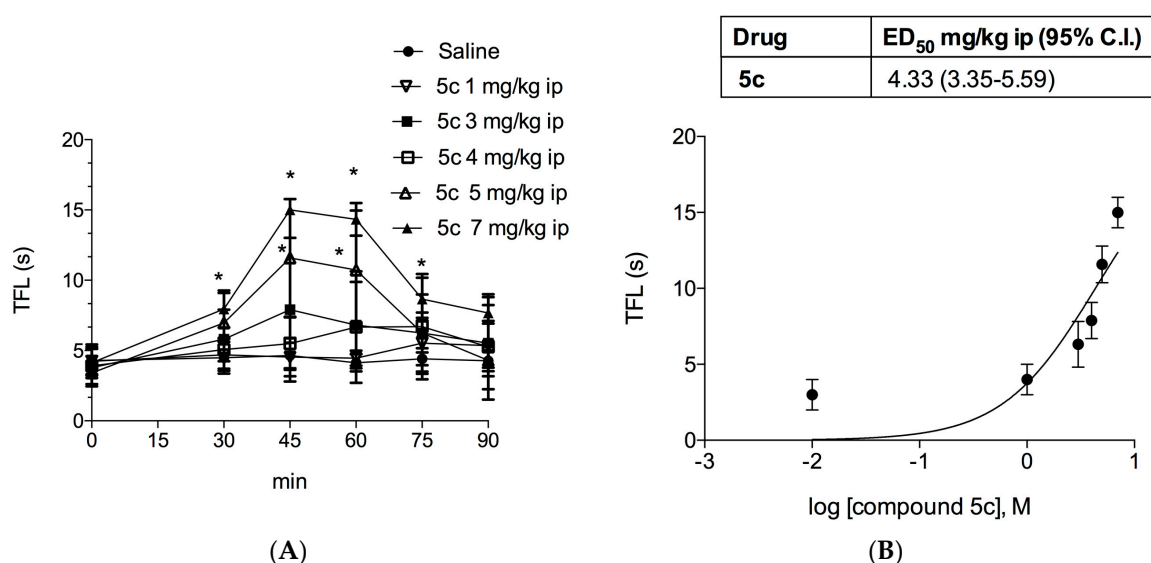


Figure 3. (A) Time-course (min) of compound 5c induced analgesia measured by tail flick latency (TFL). Results are expressed in seconds (s). Data are means \pm SEM from six to eight mice. * $p < 0.05$ vs. saline-treated mice. (B) Analgesic dose-response curve \pm SEM for compound 5c was plotted at 45 min post-treatment.

3. Discussion

In this study, our attention was focused on the evaluation of *N*-substituents in *cis*-(-)-*N*-normetazocine-based compounds to extend the knowledge about this structural region in the opioid receptor interaction. LP1 derivatives produced a pharmacological profile at MOR, DOR and KOR different one from another as consequence of the *N*-substituent nature whose flexibility allow them to reposition themselves differently relative to the *cis*-(-)-*N*-normetazocine nucleus. Moreover, the presence of a second positive charge at the *N*-substituent, as well as the shortening of the *N*-substituent spacer, seem to address the ligand-opioid receptor interaction mainly at MOR and KOR. Almost all synthesized compounds, in HEK293 cells stably expressing MOR, resulted MOR partial agonists and compound 5c exhibited an IC₅₀ value of 11.5 nM and an I_{max} of 72% with a slight lower efficacy than LP1. In tail flick test compound 5c confirmed its *in vitro* profile with an analgesic activity naloxone-reversed and an ED₅₀ of 4.33 mg/kg. Moreover, in compound 5c the second positive charge at the *N*-substituent could affect its pharmacokinetic properties and could, in part, justify its reduced antinociceptive effect compared to LP1 after systemic administration.

Our results corroborated a plethora of experimental data [5,7,8] revealing the unpredictability of pharmacological properties conferred by *N*-substituents on (-)-*cis*-*N*-normetazocine scaffold. For instance, the introduction at the basic nitrogen of an aromatic ring and/or alkyl residues linked by an *N*-acetamido spacer was detrimental for opioid receptors affinity (K_i^{MOR} 722–2930 nM, $K_i^{\text{DOR}} > 5000$ nM, K_i^{KOR} 335–5000 nM) [10]. Contrarily, aromatic ring and/or alkyl residues linked by the *N*-propanamido spacer, as well as the presence of a secondary amido group, improved opioid interaction mainly at MOR [10]. Bulkier aromatic groups, such as naphthyl, quinoline and isoquinoline rings, at the *N*-propanamido spacer, were not tolerated for interaction with the opioid receptors binding pocket mainly at DOR [16]. Moreover, the bulkier size of the *N*-substituent moved the functional profile from agonism to antagonism versus MOR [16]. A shorter and more flexible ethyl spacer with H-bonding groups at carbon 2 in *N*-substituent of (-)-*cis*-*N*-normetazocine nucleus allowed an optimal interaction with opioid binding pocket mainly at MOR and DOR [15].

4. Materials and Methods

4.1. General Experimental Procedures

All commercial chemicals were purchased from Sigma-Aldrich (St. Louis, MO, USA) or Merck (Darmstadt, Germany) and were used without further purification. (\pm)-cis-N-normetazocine was obtained from Fabbrica Italiana Sintetici (Milano, Italy). Melting points were determined in open capillary tubes with a Büchi 530 apparatus (Büchi, Flawil, Switzerland) and are uncorrected. Analytical TLC was performed on silica gel 60 F254 aluminum sheets (Merck) with fluorescent indicator. Components were visualized by UV light ($\lambda = 254$ nm) and iodine vapors. Flash column chromatography was carried out on Merck silica gel 60 (230–400 mesh). Optical rotations were determined in CHCl_3 or MeOH solution with a Perkin-Elmer 241 polarimeter (Llantrisant, UK). Infrared spectra were recorded on a 1600 FT-IR Perkin-Elmer instrument. ^1H - and ^{13}C -NMR spectra were routinely recorded on an Inova-200 spectrometer (Varian, Palo Alto, CA, USA) in CDCl_3 solution; chemical shifts δ are expressed in ppm with reference to tetramethylsilane as an internal standard. Elemental analyses (C, H, N) were performed on a Carlo Erba 1106 analyzer (Milan, Italy) and the analysis results were within $\pm 0.4\%$ of the theoretical values. All reported compounds had a purity of at least 95%. Synthesis and analytical data of compounds **1a–d**, **2a–d**, **3a–d** and **4a–d** were described in reference [10].

4.2. Chemistry

General procedure for the reduction of cis-(–)-N-substituted-N-normetazocine derivatives to afford compounds 5a–d and 6a–d. To a 1 M solution of diborane (2 mL, 2 mmol) in THF, cooled at 0 °C and under nitrogen atmosphere, a solution of the appropriate cis-(–)-N-substituted-N-normetazocine derivatives **3a–d** and **4a–d** (1 mmol) in THF (4 mL) was slowly added. The reaction mixture was refluxed for 12 h and cooled at room temperature, and 2 mL of a 6 M hydrochloric acid solution was added slowly. THF was removed by distillation at atmospheric pressure. NaHCO_3 saturated solution was added to aqueous phase, and the latter was extracted with CHCl_3 . The organic mixture was dried over anhydrous Na_2SO_4 and evaporated *in vacuo* to give the free base. The compounds **5a–d** and **6a–d** were dissolved in THF and treated with a solution of $\text{H}_2\text{C}_2\text{O}_4 \cdot 2\text{H}_2\text{O}$ in THF to give the oxalate salts as white solids. The analytical pure samples were obtained by recrystallization.

(2*R*,6*R*,11*R*)-3-(2-Anilinoethyl)-6,11-dimethyl-1,2,3,4,5,6-hexahydro-2,6-methano-3-benzazocin-8-ol (**5a**). White solid (87%); m.p. 145–146 °C; $[\alpha]_{\text{D}}^{25} = -60^\circ$ (*c* 1.0, MeOH); ^1H -NMR (CDCl_3 , free base) δ 7.13–7.06 (2H, m), 6.96–6.92 (1H, m), 6.67–6.54 (5H, m), 3.62–3.56 (1H, m), 3.42–3.01 (7H, m), 2.56–2.49 (1H, m), 2.14–1.88 (2H, m), 1.46–1.39 (1H, m), 1.29 (3H, s), 0.79 (3H, d); ^{13}C -NMR (CDCl_3 , free base) δ 156.16, 147.90, 140.24, 128.97, 128.37, 123.19, 116.38, 113.74, 112.27, 111.88, 57.95, 51.54, 45.67, 40.15, 39.32, 37.61, 34.70, 28.94, 24.26, 12.93; anal. C 64.72, H 7.21, N 6.35%, calcd. for $\text{C}_{22}\text{H}_{28}\text{N}_2\text{O} \cdot \text{C}_2\text{H}_2\text{O}_4 \cdot \text{H}_2\text{O}$ (444.521), C 64.85, H 7.26, N 6.30%.

(2*R*,6*R*,11*R*)-3-[2-(Cyclohexylamino)ethyl]-6,11-dimethyl-1,2,3,4,5,6-hexahydro-2,6-methano-3-benzazocin-8-ol (**5b**). White solid (80%); m.p. 153–155 °C; $[\alpha]_{\text{D}}^{25} = -59^\circ$ (*c* 1.0, MeOH); ^1H -NMR (CDCl_3 , free base) δ 6.89–6.85 (1H, m), 6.69–6.56 (2H, m), 2.86–2.39 (8H, m), 2.10–1.71 (8H, m), 1.31 (3H, s), 1.28–1.18 (7H, m), 0.80 (3H, d); ^{13}C -NMR (CDCl_3 , free base) δ 155.02, 142.95, 127.98, 127.42, 113.27, 112.49, 58.79, 56.98, 53.40, 45.17, 43.20, 42.13, 41.74, 36.36, 32.74, 25.81, 25.45, 24.95, 24.16, 14.08; anal. C 63.94, H 8.52, N 6.27%, calcd for $\text{C}_{22}\text{H}_{34}\text{N}_2\text{O} \cdot \text{C}_2\text{H}_2\text{O}_4 \cdot \text{H}_2\text{O}$ (450.568), C 63.98, H 8.50, N 6.22%.

(2*R*,6*R*,11*R*)-6,11-Dimethyl-{2-[methyl(phenyl)amino]ethyl}-1,2,3,4,5,6-hexahydro-2,6-methano-3-benzazocin-8-ol (**5c**). White solid (84%); m.p. 162–163 °C; $[\alpha]_{\text{D}}^{25} = -58^\circ$ (*c* 1.0, MeOH); ^1H -NMR (CDCl_3 , free base) δ 7.63–7.40 (2H, m), 7.15–6.85 (1H, m), 6.74–6.51 (5H, m), 3.33 (3H, s), 3.26–2.89 (9H, m), 2.57–2.49 (2H, m), 1.33–1.16 (1H, m), 1.29 (3H, s), 0.76 (3H, d); ^{13}C -NMR (CDCl_3 , free base) δ 156.29, 148.69, 140.53, 129.52, 128.89, 123.55, 116.93, 114.08, 112.55, 112.14, 59.09, 51.36, 48.95, 46.97, 45.71, 38.24, 35.10,

34.95, 24.47, 23.14, 13.20; anal. C 65.44, H 7.37, N 6.12%, calcd for $C_{23}H_{30}N_2O \cdot C_2H_2O_4 \cdot H_2O$ (458.547), C 65.48, H 7.47, N 6.11%.

(2*R*,6*R*,11*R*)-6,11-Dimethyl-{2-[ethyl(phenyl)amino]ethyl}-1,2,3,4,5,6-hexahydro-2,6-methano-3-benzazocin-8-ol (**5d**). White solid (85%); m.p. 158–160 °C; $[\alpha]_D^{25} = -59^\circ$ (c 1.0, MeOH); 1H -NMR ($CDCl_3$, free base) δ 7.15–7.07 (2H, m), 6.86–6.82 (1H, m), 6.63–6.47 (5H, m), 3.50–3.38 (2H, m), 3.31 (2H, q, $J = 6.8$ Hz), 2.84–2.47 (7H, m), 2.17–1.64 (2H, m), 1.42–1.07 (1H, m), 1.25 (3H, s), 1.06 (3H, t, $J = 7.0$ Hz), 0.74 (3H, d); ^{13}C -NMR ($CDCl_3$, free base) δ 155.51, 147.46, 142.20, 129.11, 127.81, 123.19, 114.93, 112.93, 111.82, 111.28, 60.74, 58.11, 51.81, 45.31, 44.39, 40.21, 39.79, 35.73, 25.23, 23.57, 13.78, 12.17; anal. C 66.17, H 7.66, N 5.95%, calcd. for $C_{24}H_{32}N_2O \cdot C_2H_2O_4 \cdot H_2O$ (472.574), C 66.08, H 7.68, N 5.93%.

(2*R*,6*R*,11*R*)-3-(3-Anilinopropyl)-6,11-dimethyl-1,2,3,4,5,6-hexahydro-2,6-methano-3-benzazocin-8-ol (**6a**). White solid (91%); m.p. 149–150 °C; $[\alpha]_D^{25} = -45^\circ$ (c 1.0, MeOH); 1H -NMR ($CDCl_3$, free base) δ 7.09–7.02 (2H, m), 6.94–6.90 (1H, m), 6.65–6.47 (5H, m), 3.41–3.36 (1H, m), 3.04–2.78 (7H, m), 2.35–2.24 (1H, m), 1.98–1.84 (2H, m), 1.84–1.65 (2H, m), 1.39–1.28 (1H, m), 1.28 (3H, s), 0.77 (3H, d); ^{13}C -NMR ($CDCl_3$, free base) δ 156.08, 148.75, 140.87, 128.95, 128.75, 128.26, 124.08, 115.69, 113.58, 112.03, 57.55, 51.35, 45.32, 40.57, 39.25, 38.50, 35.16, 24.60, 24.50, 22.85, 13.28; anal. C 65.28, H 7.54, N 6.18%, calcd. for $C_{23}H_{30}N_2O \cdot C_2H_2O_4 \cdot H_2O$ (458.547), C 65.48, H 7.47, N 6.11%.

(2*R*,6*R*,11*R*)-3-[3-(Cyclohexylamino)propyl]-6,11-dimethyl-1,2,3,4,5,6-hexahydro-2,6-methano-3-benzazocin-8-ol (**6b**). White solid (94%); m.p. 136–138 °C; $[\alpha]_D^{25} = -47^\circ$ (c 1.0, MeOH); 1H -NMR ($CDCl_3$, free base) δ 6.96–6.92 (1H, m), 6.66–6.59 (2H, m), 3.44–3.41 (1H, m), 2.97–2.88 (6H, m), 2.49–2.35 (1H, m), 2.07–1.98 (7H, m), 1.74–1.56 (3H, m), 1.43–1.28 (6H, m), 1.28 (3H, s), 1.11–1.08 (1H, m), 0.79 (3H, d); ^{13}C -NMR ($CDCl_3$, free base) δ 156.26, 140.39, 128.35, 123.30, 113.80, 112.00, 60.08, 57.70, 56.04, 55.75, 54.92, 50.13, 45.26, 41.20, 34.87, 28.51, 24.76, 24.36, 23.93, 21.02, 13.09; anal. C 64.55, H 8.64, N 6.09%, calcd. for $C_{23}H_{36}N_2O \cdot C_2H_2O_4 \cdot H_2O$ (464.595), C 64.63, H 8.68, N 6.03%.

(2*R*,6*R*,11*R*)-6,11-Dimethyl-{3-[methyl(phenyl)amino]propyl}-1,2,3,4,5,6-hexahydro-2,6-methano-3-benzazocin-8-ol (**6c**). White solid (91%); m.p. 140–142 °C; $[\alpha]_D^{25} = -52^\circ$ (c 1.0, MeOH); 1H -NMR ($CDCl_3$, free base) δ 7.19–7.12 (3H, m), 6.73–6.60 (5H, m), 3.63–3.57 (1H, m), 3.44–2.89 (7H, m), 2.85 (3H, s), 2.49–2.40 (1H, m), 2.09–1.88 (4H, m), 1.45–1.38 (1H, m), 1.28 (3H, s), 0.78 (3H, d); ^{13}C -NMR ($CDCl_3$, free base) δ 156.29, 148.88, 140.13, 129.04, 128.42, 122.99, 115.96, 113.86, 112.22, 111.99, 57.69, 49.12, 40.75, 39.91, 39.13, 39.00, 38.25, 37.73, 34.77, 24.24, 21.14, 12.92; anal. C 66.10, H 7.64, N 5.99%, calcd. for $C_{24}H_{32}N_2O \cdot C_2H_2O_4 \cdot H_2O$ (472.574), C 66.08, H 7.68, N 5.93%.

(2*R*,6*R*,11*R*)-6,11-Dimethyl-{3-[ethyl(phenyl)amino]propyl}-1,2,3,4,5,6-hexahydro-2,6-methano-3-benzazocin-8-ol (**6d**). White solid (93%); m.p. 138–139 °C; $[\alpha]_D^{25} = -55^\circ$ (c 1.0, MeOH); 1H -NMR ($CDCl_3$, free base) δ 7.18–6.92 (3H, m), 6.69–6.52 (5H, m), 3.52–3.37 (2H, m), 3.31 (2H, q, $J = 6.8$ Hz), 2.97–2.91 (4H, m), 2.64–2.45 (3H, m), 2.07–1.74 (4H, m), 1.43–1.36 (1H, m), 1.28 (3H, s), 1.06 (3H, t, $J = 6.8$ Hz), 0.79 (3H, d); ^{13}C -NMR ($CDCl_3$, free base) δ 156.16, 147.44, 140.44, 129.14, 128.32, 123.48, 115.34, 113.70, 111.95, 111.84, 57.73, 50.53, 46.80, 45.33, 44.07, 39.75, 37.89, 34.93, 25.61, 24.37, 22.56, 13.03, 11.97; anal. C 66.65, H 7.81, N 5.72%, calcd. for $C_{25}H_{34}N_2O \cdot C_2H_2O_4 \cdot H_2O$ (486.601), C 66.64, H 7.87, N 5.76%.

4.3. Receptor Binding Assays

Drugs and reagents. Radioligands [3H]-DAMGO, [3H]-DPDPE and [3H]-(+)-U69,593 were purchased by Perkin-Elmer Life Sciences (Boston, MA, USA). Naloxone hydrochloride was purchased from Tocris Bioscience (Bristol, UK).

Competitive Radioligand Binding Assay. MOR, DOR and KOR binding experiments were performed on rat or guinea pig brain membranes according to the experimental protocol described by Spetea et al. [17], as reported elsewhere [18]. Protein concentration was determined by Lowry's method using bovine serum albumin as standard [19]. Binding experiments at MOR and DOR were carried out by incubating 0.4 mg/mL and 0.5 mg/mL of rat brain membrane proteins, respectively for 45 min at 35 °C either with 1 nM [3H]-DAMGO (48.4 Ci/mM) or 2 nM [3H]-DPDPE (52.7 Ci/mM) in 50 mM

Tris-HCl (pH 7.4). Regarding KOR binding assays, guinea pig brain membranes (0.5 mg/mL) were incubated for 30 min at 30 °C with 1 nM [³H]-(+)-U69,593 (42.69 Ci/mM). Test compounds were added in concentration ranging from 10⁻⁵ to 10⁻¹¹ M. Nonspecific binding was assessed in the presence of 10 μM of unlabeled naloxone. The reaction was terminated by filtering the solution through Whatman GF/B glass fiber filters, which were presoaked for 1 h in a 0.5% polyethylenimine solution. Filters were washed with ice-cold buffer (2 × 4 mL), dried, soaked in 4 mL of “Ultima Gold MV” scintillation cocktail and counted on a Beckman LS 6500 liquid scintillation counter.

Data analysis. K_i values were calculated using the EBDA/LIGAND program (version 4) purchased from Elsevier/Biosoft (Cambridge, UK).

4.4. cAMP Accumulation Assay

Cell culture. HEK293 cells stably expressing either the EE-tagged MOR or the flag-tagged KOR [20–22] were grown in Dulbecco’s modified Eagle’s medium (DMEM) supplemented with 10% fetal calf serum, 2 mM glutamine, 100 U/mL penicillin, and 0.1 mg/mL streptomycin under 5% CO₂ at 37 °C.

Measurements of cAMP accumulation. Measurements of AC activity were performed as described by Papakonstantinou et al. [22] or the GloSensor cAMP Assay (Promega) following the Manufacturer’s instructions. The generation of cAMP was assessed in response to treatment of the cells with various concentrations of the appropriate ligand (10 pM–50 μM) using 50 μM forskolin at 37 °C. Values are means ± SD of triplicate determinations from three independent experiments. Analysis of the data was performed using Origin 7.5 software (OriginLab Corporation, Northampton, MA, USA).

4.5. In Vivo Pharmacology

Animals. Male Swiss CB1 mice (Envigo Laboratories, S. Pietro al Natisone (UD), Italy) weighing 25–30 g were housed six to a cage. Animals were kept at a constant room temperature (25 ± 1 °C) under a 12:12 h light and dark cycle with free access to food and water. Each mouse was used for only one experiment. Experimental procedures were approved by the Local Ethical Committee (IACUC) and conducted in accordance with international guidelines as well as European Communities Council Directive and National Regulations (CEE Council 86/609 and DL 116/92).

Nociceptive Test. Nociception was evaluated by the radiant heat tail-flick test [11,23]. Briefly, it consisted of irradiation of the lower third of the tail with an infrared source (Ugo Basile, Comerio, Italy). The day before the experiment, mice were habituated to the procedure for measuring nociception threshold. Experiments were performed at room temperature (25 ± 1 °C). The basal pre-drug latency was established between 3 and 5 s and was calculated as the average of the first three measurements, which were performed at 5 min intervals. A cut-off latency of 15 s was established to minimize damage to the tail. All tested compounds were dissolved in pyrogen-free isotonic saline (Baxter Healthcare, Deerfield, IL, USA) and DMSO (5%) and were administered to mice ip. Post-treatment tail flick latencies (TFLs) were determined at 30, 45, 60, 75 and 90 min after ip injection.

Statistical Analysis. All values were presented as means ± SD. Intergroup comparisons were assessed using an initial two-way analysis of variance (ANOVA) followed by Duncan’s multiple range post-hoc test. Differences were considered significant when * *p* < 0.05. Effective dose-50 (ED₅₀) values were calculated using least-squares linear regression analysis followed by calculation of 95% confidence limits (95% CL) by the method of Bliss [12,24].

5. Conclusions

This study expands the understanding on the importance of *N*-substituent structural variations in opioid receptor profile of *cis*-(-)-*N*-normetazocine derivatives and identify compound **5c** as a new MOR agonist useful for the development of novel opioid analgesics for pain treatment.

Acknowledgments: This work was supported by University of Catania (PdR 2016–2018) to Lorella Pasquinucci. The authors gratefully acknowledge Fabbrica Italiana Sintetici (Milan, Italy) for providing (±)-*cis*-*N*-normetazocine. We thank Thomas Fazio for his assistance with English language editing.

Author Contributions: R.T., C.P. and L.P. designed and performed chemistry and in vivo experiments; O.P. designed and performed the radioligand binding assays; Z.G. and P.P. designed and performed the cAMP assay; L.P., C.P., R.T., O.P., E.A. and A.M. participated in the analysis and interpretation of data. R.T., C.P. and L.P. wrote the manuscript. All the authors read and approved the final manuscript.

Conflicts of Interest: The authors declare no conflict of interest.

References

1. Williams, D.A.; Roche, V.F.; Roche, R.A. Central Analgesics. In *Foye's Principles of Medicinal Chemistry*, 7th ed.; Lippincott Williams & Wilkins: Philadelphia, PA, USA, 2012; pp. 658–699. ISBN 1609133455.
2. Janecka, A.; Fichna, J.; Janecki, T. Opioid receptors and their ligands. *Curr. Top. Med. Chem.* **2004**, *4*, 1–17. [[CrossRef](#)] [[PubMed](#)]
3. Turnaturi, R.; Marrazzo, A.; Parenti, C.; Pasquinucci, L. Benzomorphan scaffold for opioid analgesics and pharmacological tools development: A comprehensive review. *Eur. J. Med. Chem.* **2018**, *148*, 410–422. [[CrossRef](#)] [[PubMed](#)]
4. Lipkowski, A.W.; Misicka, A.; Porreca, F.; Davis, P.; Yamamura, H.I.; Stropova, D.; Hruby, V.J. Benzomorphan alkaloids: Natural peptidomimetics of opioid peptide pharmacophores. *Lett. Pept. Sci.* **1995**, *2*, 177–181. [[CrossRef](#)]
5. Aceto, M.D.; May, E.L.; Harris, L.S.; Bowman, E.R.; Cook, C.D. Pharmacological studies with a nonpeptidic, delta-opioid (–)-(1R,5R,9R)-5,9-dimethyl-2'-hydroxy-2-(6-hydroxyhexyl)-6,7 benzomorphan hydrochloride ((–)-NIH 11082). *Eur. J. Pharm.* **2007**, *566*, 88–93. [[CrossRef](#)] [[PubMed](#)]
6. May, E.L.; Aceto, M.D.; Bowman, E.R.; Bentley, C.; Martin, B.R.; Harris, L.S.; Medzihradsky, F.; Mattson, M.V.; Jacobson, A.E. Antipodal alpha-N-(methyl through decyl)-N-normetazocines (5,9 alpha-dimethyl-2'-hydroxy-6,7-benzomorphans): In vitro and in vivo properties. *J. Med. Chem.* **1994**, *37*, 3408–3418. [[CrossRef](#)] [[PubMed](#)]
7. May, E.L.; Jacobson, A.E.; Mattson, M.V.; Traynor, J.R.; Woods, J.H.; Harris, L.S.; Bowman, E.R.; Aceto, M.D. Synthesis and in vitro and in vivo activity of (–)-(1R,5R,9R)- and (+)-(1S,5S,9S)-N-alkenyl-, -N-alkynyl-, and -N-cyanoalkyl-5,9-dimethyl-2'-hydroxy-6,7-benzomorphan homologues. *J. Med. Chem.* **2000**, *43*, 5030–5036. [[CrossRef](#)] [[PubMed](#)]
8. Metcalf, M.D.; Aceto, M.D.; Harris, L.S.; Woods, J.H.; Traynor, J.R.; Coop, A.; May, E.L. The influence of esters and carboxylic acids as the N-substituent of opioids. Part 1: Benzomorphans. *Bioorg. Med. Chem.* **2008**, *16*, 869–873. [[CrossRef](#)] [[PubMed](#)]
9. Turnaturi, R.; Arico, G.; Ronsisvalle, G.; Pasquinucci, L.; Parenti, C. Multitarget Opioid/Non-opioid Ligands: A Potential Approach in Pain Management. *Curr. Med. Chem.* **2016**, *23*, 4506–4528. [[CrossRef](#)] [[PubMed](#)]
10. Pasquinucci, L.; Prezzavento, O.; Marrazzo, A.; Amata, E.; Ronsisvalle, S.; Georgoussi, Z.; Fourla, D.D.; Scoto, G.M.; Parenti, C.; Aricò, G.; et al. Evaluation of N-substitution in 6,7-benzomorphan compounds. *Bioorg. Med. Chem.* **2010**, *18*, 4975–4982. [[CrossRef](#)] [[PubMed](#)]
11. Pasquinucci, L.; Parenti, C.; Turnaturi, R.; Aricò, G.; Marrazzo, A.; Prezzavento, O.; Ronsisvalle, S.; Georgoussi, Z.; Fourla, D.D.; Scoto, G.M.; et al. The benzomorphan-based LP1 ligand is a suitable MOR/DOR agonist for chronic pain treatment. *Life Sci.* **2012**, *90*, 66–70. [[CrossRef](#)] [[PubMed](#)]
12. Parenti, C.; Turnaturi, R.; Aricò, G.; Marrazzo, A.; Prezzavento, O.; Ronsisvalle, S.; Scoto, G.M.; Ronsisvalle, G.; Pasquinucci, L. Antinociceptive profile of LP1, a non-peptide multitarget opioid ligand. *Life Sci.* **2012**, *90*, 957–961. [[CrossRef](#)] [[PubMed](#)]
13. Parenti, C.; Turnaturi, R.; Aricò, G.; Gramowski-Voss, A.; Schroeder, O.H.; Marrazzo, A.; Prezzavento, O.; Ronsisvalle, S.; Scoto, G.M.; Ronsisvalle, G.; et al. The multitarget opioid ligand LP1's effects in persistent pain and in primary cell neuronal cultures. *Neuropharmacology* **2013**, *71*, 70–82. [[CrossRef](#)] [[PubMed](#)]
14. Accolla, M.L.; Turnaturi, R.; Sarpietro, M.G.; Ronsisvalle, S.; Castelli, F.; Pasquinucci, L. Differential scanning calorimetry approach to investigate the transfer of the multitarget opioid analgesic LP1 to biomembrane model. *Eur. J. Med. Chem.* **2014**, *77*, 84–90. [[CrossRef](#)] [[PubMed](#)]
15. Pasquinucci, L.; Turnaturi, R.; Prezzavento, O.; Arena, E.; Aricò, G.; Georgoussi, Z.; Parenti, R.; Cantarella, G.; Parenti, C. Development of novel LP1-based analogues with enhanced delta opioid receptor profile. *Bioorg. Med. Chem.* **2017**, *25*, 4745–4752. [[CrossRef](#)] [[PubMed](#)]

16. Pasquinucci, L.; Turnaturi, R.; Aricò, G.; Parenti, C.; Pallaki, P.; Georgoussi, Z.; Ronsisvalle, S. Evaluation of N-substituent structural variations in opioid receptor profile of LP1. *Bioorg. Med. Chem.* **2016**, *24*, 2832–2842. [[CrossRef](#)] [[PubMed](#)]
17. Spetea, M.; Bohotin, C.R.; Asim, M.F.; Stübegger, K.; Schmidhammer, H. In vitro and in vivo pharmacological profile of the 5-benzyl analogue of 14-methoxymetopon, a novel mu opioid analgesic with reduced propensity to alter motor function. *Eur. J. Pharm. Sci.* **2010**, *41*, 125–135. [[CrossRef](#)] [[PubMed](#)]
18. Prezzavento, O.; Arena, E.; Sánchez-Fernández, C.; Turnaturi, R.; Parenti, C.; Marrazzo, A.; Catalano, R.; Amata, E.; Pasquinucci, L.; Cobos, E.J. (+)- and (–)-Phenazocine enantiomers: Evaluation of their dual opioid agonist/ $\sigma(1)$ antagonist properties and antinociceptive effects. *Eur. J. Med. Chem.* **2017**, *125*, 603–610. [[CrossRef](#)] [[PubMed](#)]
19. Lowry, O.H.; Rosebrough, N.J.; Farr, A.L.; Randall, R.J. Protein measurement with the folin phenol reagent. *J. Biol. Chem.* **1951**, *193*, 265–275. [[PubMed](#)]
20. Morou, E.; Georgoussi, Z. Expression of the third intracellular loop of the delta opioid receptor inhibits signalling by opioid receptors and other GPCRs. *J. Pharm. Exp. Ther.* **2005**, *315*, 1368–1379. [[CrossRef](#)] [[PubMed](#)]
21. Fourla, D.D.; Papakonstantinou, M.P.; Vrana, S.; Georgoussi, Z. Selective interactions of the C-termini of the δ - and μ -opioid receptor signaling. *Cell Signal.* **2012**, *24*, 2315–2328. [[CrossRef](#)] [[PubMed](#)]
22. Papakonstantinou, M.P.; Karoussiotis, C.; Georgoussi, Z. RGS2 and RGS4 proteins: New modulators of the κ -opioid receptor signaling. *Cell Signal.* **2015**, *27*, 104–114. [[CrossRef](#)] [[PubMed](#)]
23. Prezzavento, O.; Arena, E.; Parenti, C.; Pasquinucci, L.; Aricò, G.; Scoto, G.M.; Grancara, S.; Toninello, A.; Ronsisvalle, S. Design and synthesis of new bifunctional sigma-1 selective ligands with antioxidant activity. *J. Med. Chem.* **2013**, *56*, 2447–2455. [[CrossRef](#)] [[PubMed](#)]
24. Bliss, C.I. *Statistics in Biology*; McGraw-Hill: New York, NY, USA, 1967; pp. 558–639.

Sample Availability: Not available.



© 2018 by the authors. Licensee MDPI, Basel, Switzerland. This article is an open access article distributed under the terms and conditions of the Creative Commons Attribution (CC BY) license (<http://creativecommons.org/licenses/by/4.0/>).